Egypt. J. Chem. **Vol. 67**, No. 12 pp. 253 - 265 (2024)

Egyptian Journal of Chemistry

http://ejchem.journals.ekb.eg/

Statistical Optimization, Characterization and *In Vivo* Toxicity Assessment of Selenium Nanoparticles Biosynthesized by *Bacillus Halotolerans*

Basant A. Ali[1*], Amany A. Hassabo[1], Mohamed Abdelraof[1], Hala S. Hussein[2], Sahar M. Gebril[3] and Amria Mamdouh Mousa[4*]

[1] *Department of Microbial Chemistry, National Research Centre, Dokki, 12622, Cairo, Egypt*
[2] *Department of Chemical Engineering & Pilot Plant, National Research Centre, Dokki, 12622, Cairo, Egypt*
[3] *Department of Histology and Cell biology, Faculty of Medicine, Sohag University, Sohag, 82524, Egypt*
[4] *Department of Biochemistry, National Research Centre, Dokki, 12622, Cairo, Egypt*

Abstract

Selenium nanoparticles are attractive nanomaterials for application in medicine and therapeutics due to their antimicrobial and anticancer features. They are used as potential chemotherapeutic agents in a variety of cancers due to their broad range of biological activity, minimal toxicity, and prolonged effects. Therefore, the aim of this study was to optimize the biosynthesis of SeNPs using cell free extract of marine bacteria. The potent marine bacterial isolate was identified as *Bacillus halotolerans* based on 16S rRNA gene sequencing. Characterization of SeNPs by UV–Vis spectroscopy, SEM–EDX, X-ray diffraction (XRD), and TEM techniques disclosed the biosynthesis of granular and spherical shaped SeNPs with size heterogeneity averaging between 7.50 - 19.17 nm. Consequently, SeNPs preparation using cell free extract of *Bacillus halotolerans* was statistically optimized using Plackett–Burman Design. Among five selected variables, reaction temperatures followed by the cell concentration were found to be significant factors for maximal biosynthesis of SeNPs. The most significant factors were confirmed based on the calculated percentage of participation P (%) from an analysis of the variance (ANOVA), which was less than 0.05. The acute and subacute toxicity studies were evaluated in mice to screen SeNPs safety. Biochemical, hematological and histopathological analysis were investigated. SeNPs showed no acute toxicity up to dose of 2000 mg/kg. In sub-acute toxicity, no remarkable differences between the control and SeNPs treated mice groups in terms of body weight, biochemical parameters, hematological indices or microscopic appearance of liver and kidneys were observed. Therefore, our results indicate that SeNPs could be used safely as anticancer agent without any toxic risk.

***Keywords*:** Selenium nanoparticles, Biosynthesis, Microbial reduction, Optimization, Bioactivity and Acute toxicity.

1. Introduction

Selenium (Se) is a trace element that belongs to chalcogens group in the periodic table. It is called 'the controversial element' because excess Se in diet can be lethal while low amount of Se can cause chronic diseases and Se-deficiency. Zerovalent selenium (Se^0) has a potential bioactivity which can be exploited in medical applications due to its anti-cancer, antiviral and anti-oxidative properties [1]. There are various forms of selenium that differ in the appearance and physical properties such as gaseous selenide (Se^{2-}), water soluble selenite (SeO_3^{2-}), red amorphous selenium (Se^0) and colorless/water soluble selenium dioxide (SeO_2). Organic selenium has a better bioavailability with less toxicity than inorganic selenium [1].

Nanobiotechnology is overwhelming many years ago to design and manipulate different materials from atomic scale to nanoscale (1-100 nm). At this scale, materials show off novel and different properties and

*Corresponding author e-mail: basantelkady@yahoo.com.; (Basant A. Ali).
EJCHEM use only: Received date 10 September 2024; revised date 08 October 2024; accepted date 09 October 2024
DOI: 10.21608/ejchem.2024.319982.10398

applications with huge profits in wide range of biomedical applications [2]. Various metallic-based nanomaterials have been reported to be effectively applicable in a variety of fields [3–5]. Similarly, Se nanoparticles (SeNPs) has been formerly proved better bioavailability, lower toxicity, higher absorption rates by the human body, particle dispersion and large surface area than organic and inorganic selenium compounds [6–8]. Thus, SeNPs are promising nanomaterial showing strong chemoprotective activity with antidiabetic and antioxidant impacts. SeNPs also, offer excellent antimicrobial and antiparasitic effects [9]. Nevertheless, potential toxic effects of such nanomedicine must be taken into consideration, because the smaller size of the nanoparticles, the increased cellular reactivity which may induce oxidative stress or cause cellular dysfunction [10–12]. Thus, there are several studies have addressed the *in vivo* toxicity of the biogenic SeNPs [13–15].

Due to the fact that SeNPs are not stable and tend to aggregate very fast, it was important to establish an efficient method for their synthesis with high dispersion and stability rates [16]. SeNPs can be prepared chemogenically or biogenically based on the agent controlling their synthesis. In the chemogenic NPs synthesis, the reducing agent comes as a result of physiochemical reactions, while the biogenic NPs synthesis acts as biomineralization process [17]. The biosynthesis of selenium nanoparticles is considered a green and efficient method for large scale SeNPs production compared to the chemical and physical synthesis methods [18]. Plant extracts, algae, fungi, bacteria and yeasts are the common sources for providing simple, low cost, non-toxic, eco-friendly method for SeNPs biosynthesis [19,20]. The microorganisms are promising bio-factories that capable of conversion of selenium salts to biologically active SeNPs [21]. The microorganism reduces the high-valence Se into SeNPs capped with different biomacromolecules (proteins, lipids and polysaccharides) which elevate the nanoparticles stability [1]. This process is accomplished in four stages; 1. Transport of selenium oxyanions into the cell, 2. Redox reactions takes place, 3. Export of selenium metal out of the cell and finally, 4. Assembly of Se metal into SeNPs. According to the localization of the redox reactions and SeNPs formation (either extracellular, intracellular or periplasmic), stages 1 and 3 are defined [22].

Most of the present research focuses on the study of high-yield strains and molecular mechanisms, scalability of the nanoparticles was not covered enough. Bioreactor scale fermentations can overcome some issues such as poor mixing and unbalanced nutrition, that is associated with small shake flask fermentation. In this concern, Wang et al., (2024) optimized the fermentation parameters for the biosynthesis of SeNPs by *Bacillus licheniformis* using response surface methodology. The optimized process increased the quantity of bacterial cells and production of SeNPs providing fundamental data for large-scale SeNPs fermentation [23].

There are many reports addressed the bacterial SeNPs synthesis such as lactic acid bacteria [24,25], probiotic *Bacillus* subtilis BSN313 [26], marine bacteria *Pseudoalteromonas shioyasakiensis* [27] and *Bacillus amyloliquefaciens* [28]. *Bacillus* sp. has gained attention due to its strong selenium tolerance and ability to synthesize SeNPs. It can still reduce SeNPs even at high sodium selenite concentrations, suggesting a better selenium tolerance than some other reported bacteria such as *Pseudomonas moraviensis* [29], *Vibrio natriegens* [30]. Moreover, biosynthesis of SeNPs by *B. subtilis* is accompanied by a significant increase in the accumulation of proteins. It was significant since *Bacillus* species are thought to be the main producers of bioactive secondary metabolites. While *lactobacilli*, for instance, produce significantly lower level of bioactive compounds compared to *Bacillus* species [31].

In the presented study, SeNPs was biologically synthesized using cell free extract of a marine bacterium, *B. halotolerans*, using selenium dioxide as selenium precursor. Subsequently, the biosynthesized SeNPs were characterized by different techniques, including UV–Vis spectroscopy, XRD, SEM and TEM. Statistical optimization of biosynthesized SeNPs was carried out using Plackett–Burman Design. Finally, we assessed the potential toxicity of the biosynthesized SeNPs by evaluating their acute and sub-acute toxicity in mice to confirm their safety for subsequent *in vivo* applications.

2. Experimental

Chemicals

YPD broth medium (Yeast-Peptone-Dextrose) was used for inoculum preparation. Selenium dioxide was purchased from Loba Chemie Pvt. Ltd., India. All other chemicals were obtained from NRC laboratory.

Microorganism

Marine isolate was obtained from beach sand of the Mediterranean-Sea, Alexandria- Egypt (31°11′51″N 29°53′33″E). Isolation of marine microbiota was conducted according to literature [32].

Methods

16S Ribosomal RNA (rRNA)-based Molecular Identification

Bacterial isolate was propagated in Luria-Bertani broth (LB). A 24 h grown culture was centrifuged at 12,000 g for 5 min and collected after resuspension in 0.85% NaCl for three times. Extraction of genomic DNA was performed using Gene JET Genomic DNA purification kit (Thermo Scientific, Lithuania). PCR amplification, purification, and sequencing were performed using a protocol of Macrogen Company (Seoul, South Korea; https://www.macrogen.com).

Amplification was accomplished by forward primer 8F (5′-CAG GCC TAA CAC ATG CAA GTC-3′) and reverse primer 1492R (5′-GGG CGG GGT GTACAA GGC-3′). The PCR mixture (50 µl) contained; 25 µl of DreamTaq Green DNA Polymerase (Thermo Fisher Scientific, USA), 22 µl of MQ, one µl of each forward and reverse primer (10 µmol/l) and one µl of template. PCR amplification was conducted as follows; preheating at 95°C for 4 min, denaturation at 95°C for 30 s, primer annealing at 50°C for 45 s, extension at 72°C for one min and final post cycling extension at 72°C for 10 min for 35 cycles. All the mentioned reactions were performed in a thermal cycler (Applied Biosystem Thermal Cycler, USA).

Amplified PCR product was purified and sequenced at Macro gene, Korea. Raw data of sequencing were edited (contig and peak chromatogram verification) using the Finch T.V 1.4.0 program. Analysis of 16S rRNA sequences of strain was performed using the BLAST (N) program of the National Center of Biotechnology Information (NCBI) (Rockville Pike, Bethesda MD, USA). The phylogenetic analysis of Taxa was conducted using Molecular Evolutionary Genetic Analysis Software (MEGA version 11). To align the sequences of identified phylogenetic neighbors with the strains' representative sequences, clustalW, in the MEGA 11, was used [33]. Neighbor-joining method was applied to create the phylogenetic tree with 1000 bootstrap replications to test nodal support in the tree. The bacterial isolate of the study has its 16S rRNA gene sequence deposited in the NCBI/GenBank nucleotide sequence database with accession number PQ206509.

Microbial cultures and preparation of the whole-cell lysate

Pre-cultures were prepared in 50 ml of YPD medium. The inoculated flasks were incubated for 24 h at 30°C and 180 rpm. One milliliter of pre-culture was used to inoculate the main cultures which contain 50 ml of YPD medium. The main cultures were incubated for 48 h at 30°C and 200 rpm. Whole-cell lysate was prepared by centrifugation of the main culture at 4°C, 15,000 ×g for 10 min. (Hettich Universal, 320 R, Tuttlinger, Germany). After cell wash, the cell pellet was suspended in 10 ml sodium citrate buffer (50 mM), pH 7.0. The cell whole-cell lysate was prepared either by heat treatment of the cell suspension at 50°C for 1h or by mechanical disruption of the cell suspension using Ultrasonic Probe Sonicator (Bandelin electronic GmbH, SonopulsGM2200, Germany) at 60 MHz frequency/50 W for three cycles, 30 s each. In both cases, the whole-cell lysate was finally obtained by centrifugation at 4°C, 15,000 ×g for 10 min.

Bacterial synthesis of SeNPs

The standard procedure for SeNPs biosynthesis was performed as follow; whole-cell lysate was incubated in a 1 mM SeO_2 solution while control sample contains only the whole-cell lysate without selenium precursor. After 72 h of reaction incubation at 37°C and 200 rpm, the reaction mixture was centrifuged at 3000 rpm for 15 min. The supernatant containing SeNPs was collected, dried at 95°C for 6 h until turned into powder. Finally, SeNPs powder was calcinated at 300°C for 3 h.

Statistical optimization of SeNPs preparation

The statistical optimization of the biosynthesis of SeNPs using *Bacillus halotolerans* has been accomplished in four successive stages; Plackett-Burman experimental design (PBD), practical experiment, data analysis and results validation [34].

The production and statistical optimization of SeNPs by *Bacillus halotolerance* has been applied in four sequential steps; Plackett Burman experimental design, doing the experiment, data analysis and validation of the results [34]. Before statistical modelling, the different factors were tested for the optimum maximum and minimum levels of study based on One-factor-at-a-time method (data not shown). The medium components before optimization and conditions were checked for higher SeNPs production, and then were considered for further optimization studies. Modeling of SeNPs by *Bacillus halotolerance* has been carried out using Plackett-Burman factorial design (PBD). Table (1) shows the PBD with five numerical independent; Reaction Temp., Reaction time, Selenium conc., Cells amount and Temperature of treated cells. The design was composed of 20 experimental runs; one run was performed at the center point values. Every one of the remaining runs was conducted at two levels: upper (‘high, +’) and lower (‘low, -’) levels of all variables, Minitab 7 software (Stat-Ease Inc., Minneapolis, MN, USA, version 7.0.0) have been used.

To determine in the PBD whether the maximum production was obtained at a lower or higher concentration of the variables, two levels were used

to be compared with the experimental data performed at the center point values.

The following equation was used to estimate the experimental responses by first order model;

$$Y = \beta 0 + \sum \beta i x i$$

Where Y is the response for SeNPs biosynthesis, B_o is the model intercept and β_i is the linear coefficient, and x_i is the level of the independent variable. A first-order model might be derived from the regression results of a fractional factorial experiment based on the Stat-Ease analysis. This model is used to evaluate and screen important factors and describes the interaction among them which affect the response. The following equation was used to find out the main effect of each variable;

$$Exi = (\sum Mi + - \sum Mi-)\, N$$

Where E_{xi} is the variable main effect, ΣM_{i+} is the sum total of the response values at high level; $\Sigma Mi-$ is the sum total of the response values at low level. N is the no. of runs. Analysis of variance (ANOVA) and Minitab 17-software (version 17.0.0) were used for design the PBD.

Table 1: PB design

Factor	Name	Units	Low	High	Mean
A	Reaction Temp.	°C	30	40	0.25
B	Reaction Time	h.	24	72	3
C	Se Conc.	M	$5x10^7$ (0.5)	$8.5/10^4$ (2.2)	7
D	Cells amount	%	0.5	2	3.5
E	Temperature of Treated cells	°C	45	60	2.5

Characterization of SeNPs

The green synthesis of SeNPs was physically analyzed to investigate their size and shape. Color change of the selenium reaction mixture was monitored by visual observation and by absorbance measurement using UV-Vis spectrophotometer (Hitachi U-2900). The spectrum of the plasmon surface resonance (SPR) was recorded at wavelength range 400 - 700 nm. SEM was carried out using a Quanta Inspect S (FEI Company, Eindhoven, the Netherlands) provided with an energy-dispersive X-ray analyzer (EDX, Quanta 200) utilizing a Cu–Kα source with a post-sample Kα filterant with a scanning speed of 1 s/step and a resolution of 0.05^o/step. The mineral structure of the powdered SeNPs was ascertained by X-ray diffractor (XRD) and recorded on a Philips PW 1050/70 diffractometer (Philips, the Netherlands). JEM-HR-2001 model (JEOL, Akishima, Japan) was used for TEM analysis with 200 kV accelerating voltage to determine the particle sizes of biosynthesized SeNPs. Zeta-potential measurement was made using a Zetasizer analyzer (Malvern Zetasizer Nano ZS, from Malvern Instruments Ltd., UK) for the colloidal solution containing SeNPs. A He–Ne laser lamp (0.4 mW) with a wavelength of 633 nm was linked to the analyzer. The procedure was carried out using the dynamic light scattering (DLS) technique in an isolated chamber at 25°C.

In Vivo toxicity studies

Animals and experimental design

Six weeks old Swiss albino mice were collected from the animal house of National Research Centre, Egypt. Animals were chosen to be within a weight range of 20-21 g. Mice were housed in polycarbonate cages under standard conditions of temperature 23 ± 2°C and humidity on a light/dark cycle of 12 h. Mice were fed commercially available standard pellet *ad libitum* and had free access to distilled water. All animals received humane care in compliance with The Principles of Laboratory Animal Care. The experimental procedures were approved by the Medical Research Ethics Committee of the National Research Centre with number (13010118-1) as reported by the provisions of the relevant Egyptian laws and with relative guidelines for animal experimentation of the Helsinki Declaration.

Acute toxicity study

In acute toxicity test of SeNPs, a total of 24 mice was randomly divided equally into 6 groups. Each group was administered a single fixed dose with injection volume of 0.5 ml by the intragastric route of administration in a stepwise procedure (50, 100, 200, 400, 800, 2000 mg/kg body weight). The animals were monitored closely within 4 h of treatment and after 24 h for any signs of toxicity (behavioral and clinical signs). The evaluation of behavioral and clinical signs was standardized according to Habriev et al. [35]. Specifically, behavioral signs such as motor activity, and response to stimuli were noted and scored from no effect to moderate to severe effect, if found. Additionally, clinical signs such as lethargy, respiratory distress, twitching, convulsions, tremors, excitability, diarrhea, salivation, and coma were also monitored similarly. Thereafter, observations were made daily for 14 days. After that, all mice were humanly sacrificed, and macroscopic analysis of the internal organs was performed.

Sub-acute toxicity study

Subacute toxicity study was carried out to evaluate the adverse impacts of SeNPs on the vital organs as well as hematological and biochemical parameters following a treatment period of 4 weeks in mice.

Eighteen mice were randomly divided into three groups with 6 mice per group. The first group (control) was received vehicle only (PO), the second and the third groups were orally administrated SeNPs at the doses of 4, and 10 mg/kg, respectively, for 28 consecutive days. The animals were under supervision to notice any sign of toxicity while their weights were recorded on weekly basis. Finally, mice were anaesthetized with ketamine and xylazine (50 mg/kg and 5 mg/kg, respectively) and blood was collected. For hematological studies, blood samples were collected into ethylenediamine tetraacetic acid (EDTA) anticoagulant tubes from the retro-orbital vein. A fully automated hematology analyzer (Medonic M32, Sweden) was used for hematologic analysis. For biochemical analysis, blood samples were collected without EDTA anticoagulant and serum was then collected by centrifugation at 3000 rpm for 15 min. Aspartate aminotransferase (AST), alanine aminotransferase (ALT), total protein (TP), and albumin (ALB), Blood urea nitrogen (BUN) and creatinine (CR) were performed using Spectrum Diagnostics kits, (Egypt). The manufacturer's instruction was followed.

Following blood collection, the mice were sacrificed and vital organs (livers and kidneys) were harvested, cleaned with saline, weighed and fixed in neutral buffered 10% formalin solution for 72 h. Then such organs washed in ascending graded ethanol and subsequently embedded in paraffin wax. Four µm thickness paraffin sections were further prepared for staining with hematoxylin and eosin (H&E) according to the generally accepted method [36] then examined microscopically for general histopathological examinations.

Statistical analysis

The result figures in this work were presented using Microsoft Excel. The particle size from TEM micrograph was calculated using 4 pi software. Results of the *in vivo* toxicity study were performed by SPSS program version 16. One-way ANOVA procedures were used for Analysis of variance, followed by Tukey's post hoc test. The significance level was set at $P < 0.05$. Data were expressed as the mean ± SD.

3.Results and Discussion

Molecular identification of the bacterial isolate

The 16S rRNA sequence was matched with previously published 16S rRNA sequences of bacteria in the NCBI databases using BLAST. Selected sequences of other microorganisms with the greatest similarity to the 16S rRNA sequences of the bacterial isolate were extracted from the nucleotide sequence databases and aligned generating the phylogenetic tree.

The evolutionary history was inferred using the UPGMA method. The optimal tree is shown. The percentage of replicate trees in which the associated taxa clustered together in the bootstrap test (1000 replicates). The tree is drawn to scale, with branch lengths in the same units as those of the evolutionary distances used to infer the phylogenetic tree. The evolutionary distances were computed using the Maximum Composite Likelihood method and are in the units of the number of base substitutions per site. The proportion of sites where at least 1 unambiguous base is present in at least 1 sequence for each descendent clade is shown next to each internal node in the tree. This analysis involved 27 nucleotide sequences. All ambiguous positions were removed for each sequence pair (pairwise deletion option). Evolutionary analyses were conducted in MEGA11. Based on the 16S rRNA gene sequence with BLAST in the GeneBank database, the isolated bacterial strain used in this research belongs to the genus ***Bacillus***. The phylogenetic tree was created using the neighbor-joining method and results disclosed that the isolate is jointly relevant to ***Bacillus halotolerans*** (Fig. 1). Therefore, ***B. halotolerans*** was approved as the strain of the study.

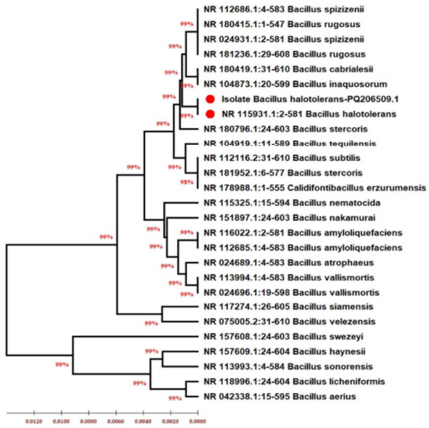

Figure 1: Phylogenetic tree based on partial 16S rRNA sequences, showing the relationship between isolate *Bacillus halotolerans* strain and other species belong to the genus *Bacillus.* The tree was constructed using the MEGA11 and neighbor-joining method.

Morphological and structural characteristics of SeNPs

SEM and EDX Study

In the present work, the biosynthesis and characterization of SeNPs were undertaken. As shown in Fig. 2A, a maximum absorbance of the biosynthesized SeNPs was shown at 565 nm. Moreover, scanning electron microscopy (SEM) (Fig. 2B) and energy dispersive X-ray (EDX) (Fig. 2C) were shown. The micrograph shows the presence of

particles with a significant heterogeneity in size. The particles of selenium were granular in shape with wide distribution. Further inspection of these particles, the EDX analysis confirmed that they were composed of elemental Se (Fig. 2C) which guarantees good synthesis of SeNPs. The elemental composition of the sample contains selenium, carbon, oxygen, potassium and sodium. The EDX spectrum of SeNPs confirmed the presence of Se (34.31%). In addition, some other signals of C (33.49%), O (23.75), and Na (7.73) were also observed which may be attributed to the grid coating. Carbon and other elements could also be derived from and the biomolecules capping the nanoparticles such as proteins and membrane phospholipids [37,38].

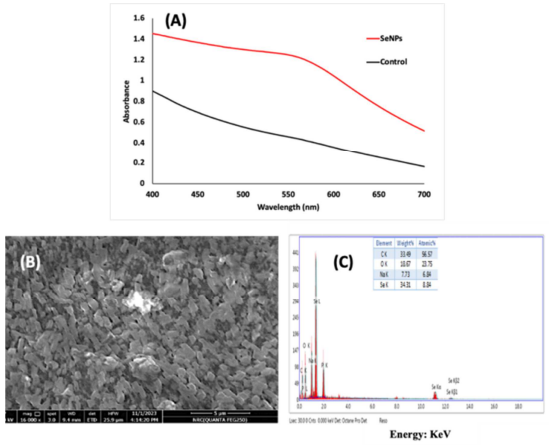

Figure 2: UV-vis spectra of the biosynthesized SeNPs (A). SEM-EDX analysis of the selenium nanoparticles (B & C respectively)

Transmission electron microscopy (TEM) Study

The transmission electron micrographs of biosynthesized SeNPs is illustrated in Fig. 3. It showed a wide range in the particle size distribution as the diameter of particles ranged from 7.50 nm to 19.17 nm. In connection, it was formerly reported by Shakibaie et al. that most marine bacterial SeNPs were in a size range 80-220 nm which is bigger than what we obtained in this study [39]. Kora obtained SeNPs biosynthesized by *Bacillus cereus* AJK3 that ranged in size from 50 to 150 nm [40].

Furthermore, the zeta potential continues to be the primary determinant of the stability of the colloidal dispersion of nanoparticles. It indicates the effective electric charge present on its surface. Since there is stronger electrostatic repulsion between the nanoparticles where the nanoparticles with bigger Zeta potentials demonstrate greater stability [41]. A shown in Fig. 3B, zeta potential for SeNPs was determined to be -37.53 mV. In a former study for Ulla et al. (2021), they isolated spherical SeNPs from *B. subtilis* with a zeta potential of -26.9 mV, suggesting that these nanoparticles easily produced and aggregated quickly in the solutions to form a stable dispersion [42].

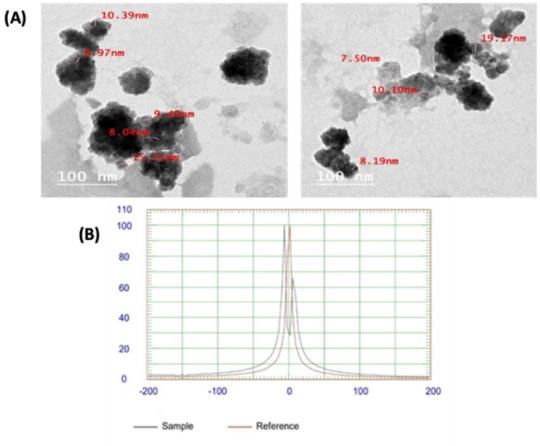

Figure 3: TEM analysis of biosynthesized SeNPs. (A). Zeta potential distribution (mV) (B).

X-ray diffraction (XRD) analysis

X-ray diffraction was used to ascertain the crystalline phase nature of the produced SeNPs, as illustrated in Fig. 4. The primary peaks of crystalline Se are visible in the acquired XRD patterns at 2θ values of 23.5°, 29.7°, 41.4°, 43.7°, and 45.4°, which correspond to the crystal planes (100), (101), (110), (102), and (111), respectively [43,44]. The obtained results showed that biosynthesized SeNPs in this study are composed of crystalline Se with high purity.

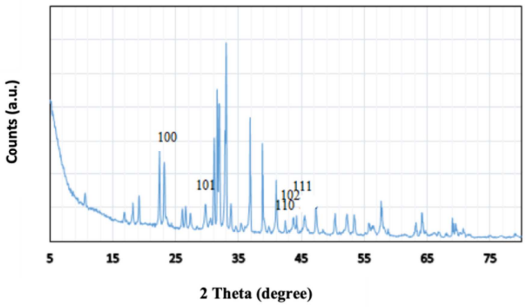

Figure 4: X-ray diffraction pattern of SeNPs.

Improvement of the SeNPs synthesis by *B. halotolerans* using Plackett-Burman design (PBD)

Factorial analysis (Plackett-Burman design) was applied in this study as an advanced statistical design to enhance the bioprocessing efficiency. PBD design was implemented in this study after determination of the most significant independent parameters by the conventional method, OFAT (data not shown). In this regard, different cultural conditions that affect SeNPs biosynthesis by *B. halotolerans* were studied as autonomous factors with their respective high and low levels.

Table 2: Optimization of the SeNPs production using Plackett-Burman design (PBD)

Run Order	Reaction Temp. (A)	Reaction Time (B)	Se Conc. (C)	Cells amount (D)	Temperature of Treated cells (E)	Response SeNPs O.D.	Fits
1	30	24	0.5	0.5	45	1.47407	1.73382
2	40	24	2.2	2.0	45	2.72149	2.48117
3	30	24	0.5	0.5	60	2.34080	1.95103
4	40	24	0.5	2.0	60	3.12234	2.87174
5	30	72	0.5	2.0	45	2.23640	2.14696
6	30	24	2.2	2.0	45	1.49259	1.98827
7	40	72	0.5	0.5	60	2.64811	2.42926
8	30	72	2.2	2.0	60	1.78692	2.19082
9	30	72	0.5	2.0	60	2.23947	2.36417
10	40	72	0.5	0.5	45	1.74748	2.21205
11	30	72	2.2	0.5	60	1.63042	1.76301
12	40	24	2.2	2.0	60	2.55211	2.69838
13	30	24	2.2	0.5	60	1.82637	1.77768
14	30	24	0.5	2.0	45	2.40085	2.16163
15	40	72	2.2	2.0	45	2.90366	2.46650
16	30	72	2.2	0.5	45	2.19530	1.54580
17	40	72	0.5	2.0	60	2.77087	2.85707
18	40	24	2.2	0.5	60	2.25632	2.27057
19	40	72	2.2	0.5	45	1.85570	2.03869
20	40	24	0.5	0.5	45	1.44490	1.60032

Results obtained from PB design showed significant variations of SeNPs production ranging from 3.1 to 1.4 O.D. in 20 runs (Table 2). These variations with shown units confirm the importance of medium optimization to obtain high productivity of SeNPs by *B. halotolerans* if compared with the SeNPs in case of OFAT (1.8 O.D.) after statistical optimization previously [34]. In addition, the Pareto chart emphasized the significance order of the factors influencing SeNPs production (Fig. 5). Among these variables, reaction temperatures followed by the cell concentration showed the maximum significance by showing the most promising effect followed by the temperature of treated cells. On contrary, SeNPs yield was not influenced by the Se concentration and the reaction time (p value >0.05).

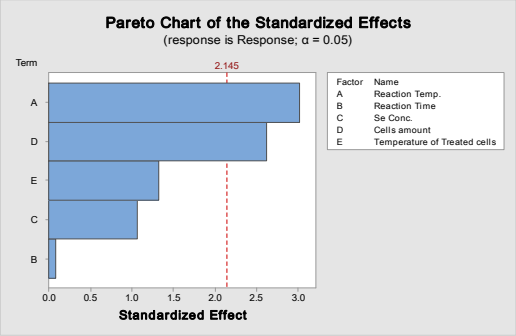

Figure 5: Pareto chart of various factors affecting SeNPs production. Factors exceeding the red line are the most promising influencing factors

In general, these findings confirmed the contribution of each significant parameter as follow; reaction temperature (42.05%), cell concentration (30.2%), temperature of the treated cells (22.5%) and Se concentration (5.6%), respectively. In addition, the significant parameters (reaction temperature and cell amount) observing P values < 0.05 significance level, which obtained by regression analysis. While the other parameters had contribution values of < 1%. To summarize, the greatest levels of the parameters as we got from response optimizer validation software are; reaction temp. of 40°C, reaction time for 24 h, Se conc. of 0.5 mM, cells conc. of 2% and temperature

of treated cells of 60°C (Fig. 6). In spite of the lower effectiveness of Se concentration on SeNPs yield, a mild significant interactive effect of Se concentration and reaction temperature was noted on SeNPs (Fig. 7). Similarly, Wang et al. (2024) found that the optimum temperature of 37°C was crucial for obtaining significant amounts of SeNPs by fermentation with *B. licheniformis* using response surface methodology [23]. Increasing the temperature to 37°C enhanced the synthesis of SeNPs by *Acinetobacter* sp. [45]. Furthermore, it was mentioned that the concentration of the bacterial cells has an impact on the efficiency and rate of SeNPs production [26]. As reported in the previous literature, the cellular extract obtained from *Azoarcus* sp. was used to generate SeNPs after 24 h of incubation [46].

Data obtained from the analysis of variance for the experiment design of SeNPs revealed that, the Model F-value of 3.80 suggests the design is close to be significant. Moreover, significant model terms were A and D where "Prob > F" less than 0.05. On the other hand, the "Pred R-Squared" of 93.7% is consistence agreement with the "Adj R-Squared" of 88.9 (Table 3).

Table 3: ANOVA of PBD experiment

Source	Sum of Squares	df	Mean Square	F-Value	p-value Prob> F*
Model	2.51708	5	0.50342	3.80	0.022
A- Reaction Temp.	2.51708	1	0.50342	9.18	0.009
B- Reaction Time	1.21474	1	1.21474	0.01	0.929
C- Se Conc.	0.00108	1	0.00108	1.14	0.305
D- Cells amount	0.15026	1	0.15026	6.92	0.020
E- Temperature of Treated cells	0.91510	1	0.91510	1.78	0.203
Curvature	1.6847	1	1.6847	4.39	0.048
Lack of Fit	15.6403	14	1.2031	9.42	0.311
Pure Error	1.85254	5	0.13232		
Cor Total	4.36962	19			

R^2=0.931; Adj R^2=0.88. df degrees of freedom; *Values of "Prob > F" less than 0.0500 indicate model terms are significant.

The initial order model equation initiated by PBD demonstrated the dependency of SeNPs biosynthesis on the medium components as follow;

Regression Equation of SeNPs yield =

$$(-0.481 + 0.0493\ Reaction\ temp - 0.00031\ Reaction\ time - 0.1020\ Se\ Conc + 0.285\ Cell\ amunt + 0.0145\ Temp\ of\ treated\ cells)$$

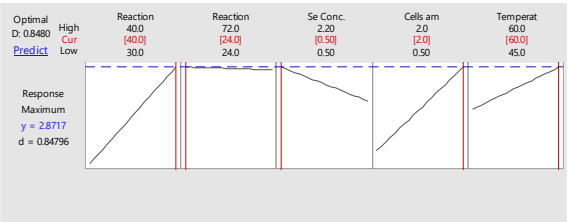

Figure 6: Response optimizer for SeNPs production by *B. halotolerans*.

The Contour charts surface response created using Minitab-17 software and indicated in (Fig. 7) were clearly exhibited the influence and validity of the different parameters on SeNPs biosynthesis. Predication of the potent variable levels for highest SeNPs production was implemented after analysis of presented charts, which was combined with numerical escalation for each variable and desirability analysis

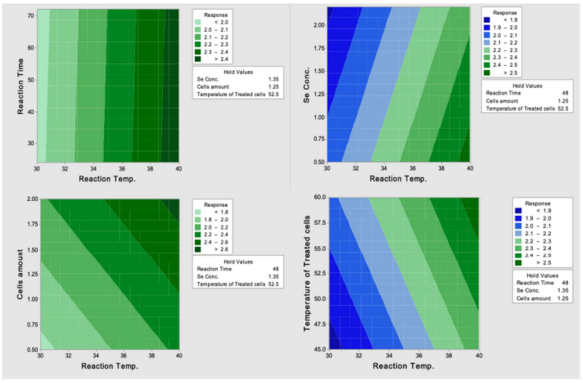

Figure 7: Contour charts of factors affecting SeNPs production.

In vivo toxicity studies

Balancing drug toxicity and its bioactivity is a major obstacle that hinders its application. Thus, the acute and sub-acute toxicities of SeNPs as well as the main procedures used to determine the possible hazards of short-or long-term exposure have been investigated [2]. In the present acute toxicity study, the administrations of SeNPs until 2000 mg/kg body weight revealed no signs of toxicity or mortality. All the mice were healthy showed normal behaviors. Postulating that, LD_{50} of the biosynthesized SeNPs is more than 2000 mg/kg and can be considered to be relatively safe without toxic effects. This is according to the Globally Harmonized System of Classification and Labelling of Chemicals [47].

We further studied the sub-acute toxicity to ensure SeNPs safety. All mice were healthy with no mortality showing a normal appearance and behavior during the 28-day experimental period. Remarkably, none of the studied parameters showed any significant adverse effects in the treated groups. It is well identified that the first sign of Se intoxication is the retardation in animals' growth [2]. As shown in Fig. 8, the weekly body weights of mice treated with SeNPs, for both doses, were lower throughout the experimental period in comparing to control group. However, it is a non-significant ($p > 0.05$) decrease in the total body weight. It was reported that selenium may influence thyroid hormone levels, which are crucial for regulating metabolic rate and potentially contribute in weight loss [48]. Moreover, the antioxidant properties of selenium may impact metabolic pathways by reducing oxidative stress and enhancing cellular function, potentially leading to changes in energy utilization that could affect body weight [49].

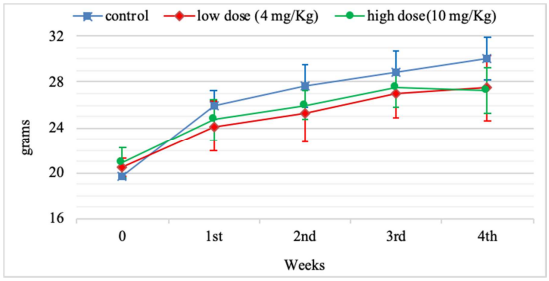

Figure 8: Effect of SeNPs on the weekly mean body weight of treated mice in comparing to control over the 28-day experimental period.

The subacute toxicity of SeNPs was tested by investigating the hematological indices as relevant indicators for possible health risks. The hematological parameters showed only a slight increase in the RBCs and platelet count in the treated groups over the control. The increase in RBCs and platelet counts in the groups treated with SeNPs compared to the control group may suggest several beneficial effects of SeNPs on blood cell production and function. First of all, the increased RBCs count indicate enhanced erythropoiesis (red blood cells production), this could lead to improved oxygen transport capacity and overall better physiological function this is due to the well-known selenium antioxidant properties, this mitigates oxidative stress, thereby supporting erythropoietic activity and regulating red cell homeostasis [50].

Moreover, selenium can stimulate hematopoietic stem cells within the bone marrow, promoting the differentiation and proliferation of precursor cells into mature RBCs and platelets. This stimulation can enhance the overall blood cell production, contributing to the observed increases in both RBCs and platelets [51].

The other hematological biomarkers were at normal ranges without statistically significant differences from the controls, shown in in Table (4).

Table 4: Effect of SeNPs on hematological values of treated mice in comparing to control group

Parameters	Control	SeNPs (4 mg/kg)	SeNPs (10 mg/kg)
RBC (x10^{12}/L)	7.99±1.74	8.89±0.55	8.71±0.70*
HB (g/dl)	13.65±1.80	14.12±1.27	14.45±0.67
HCT (%)	39.55±7.39	42.12±3.87	43.27±1.89
MCV (fl)	48.56±1.99	47.07±1.94	49.75±2.14
MCH (pg)	16.30±0.62	15.8±0.62	16.62±0.64
MCHC (g/dl)	33.60±0.10	33.62±0.42	33.4±0.36
RDW-CV (%)	14.1±0.8	15.5±0.33	15.37±0.4
RDW-SD (fl)	32.33±1.87	32.78±2.13	34.3±2.14
PLT (x10^{9}/L)	623.10±52.70	687.25±24.26	701.5±51.66*
MPV (fl)	5.75±0.34	5.65±0.12	5.45±0.25
P-LCR	4.375±2.02	4.875±1.19	4.45±1.0
PDW	8.45±0.38	8.35±0.12	8.30±0.45
WBC (x10^{9}/L)	5.12±0.58	5.175±1.89	4.9±0.39
LYM (x10^{9}/L)	4.15±1.28	4.025±1.7	3.35±0.20
GRAN (x10^{9}/L)	0.20±0.08	0.32±0.05	0.30±0.08

All data are given as mean ± SD. *p < 0.05, significantly different when compared with control. RBC=red blood cells; HB=hemoglobin; HCT= hematocrit; MCV= mean corpuscular volume; MCH= Mean Corpuscular Hemoglobin; MCHC= mean corpuscular hemoglobin concentration; RDW-CV= coefficient of variation in red cell distribution width; RDW-SD= standard deviation in red cell distribution width; PLT= Platelets; MPV= mean platelet volume; PCV= packed cell volume, P-LCR= platelet large cell ratio; PDW= platelet distribution width; WBC= white blood cell count; LYM = lymphocyte count; GRAN= granulocyte count.

Moreover, the effect of the biosynthesized SeNPs was investigated on the liver as one of the major organs largely susceptible to toxicity. It was found that the liver weight in the high-dose treated group was less than that of the control group. However, this decrease had no toxicological significance (Fig. 9A). While the liver index was not affected (Fig. 9B). Also, liver biochemical indices, assayed as indicators of liver toxicity, showed that ALT, AST, TP, and ALB levels in both low and high-dose groups were non-significantly changed from those of the control group (Fig. 9C- 9F).

It is worth noting that TP levels were significantly increased in high SeNPs group than that of the control group, yet this has no toxicological meaning. Furthermore, histological examination of liver (Fig. 9G) demonstrated that low and high-dose groups have no pathological variations when compared to the control group. It confirms that the biosynthesized SeNPs caused no noticeable histological damage to the mice liver within the 28-days experimental period. Such result is the same as that of Zhang et al [2]. Besides, previous studies showed that SeNPs have hepatoprotective effects [52,53].

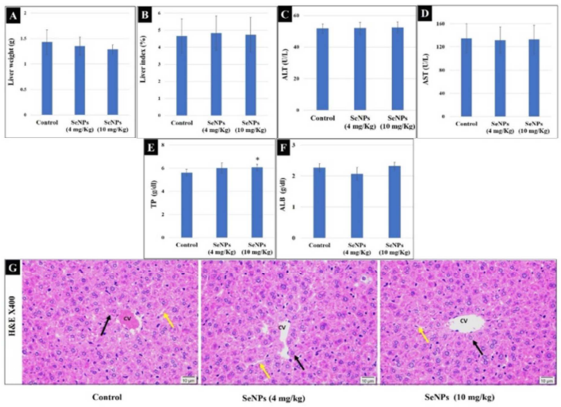

Figure 9: Effect of SeNPs (4 mg and 10 mg/kg body weight) on mice liver in comparing to control group. **(A)** Effect of SeNPs on the liver weight. **(B)** Effect of SeNPs on the liver index. **(C-G)** Effect of SeNPs on liver function parameters. **(H)** Photomicrographs obtained by light microscopy illustrating liver tissue stained with H&E. The control group, SeNPs(4 mg/kg) group and SeNPs (10 mg/kg) group, show almost normal hepatic histological organization comprising a central vein (CV) and emitting plates of liver cells (black arrow). The plates are segregated by blood sinusoids (yellow arrow). (Scale bar:10 µm).

In addition, it was found that the kidney weight and kidney index in the treated groups was not affected (Fig. 10A and 10B). Also, BUN and CR levels, valuable screening parameters in evaluating

kidney function, were found to be non-significantly changed from those of the control group (Fig. 10C-10D).

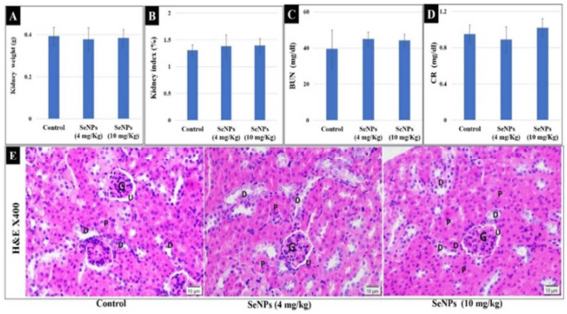

Figure 10: (A) Effect of SeNPs on the kidney weight, **(B)** Effect of SeNPs on the kidney index of treated mice in comparing to control group. **(C-D)** Effect of SeNPs on blood urea nitrogen and creatinine. **(E)** Photomicrographs obtained by light microscopy illustrating kidney tissue stained with H&E. The control group, SeNPs (4 mg/kg) and SeNPs (10 mg/kg) groups show almost normal histological organization comprising; the kidney cortical tissue renal corpuscles that consist of a glomerular capillary tuft (G) enclosed by the urinary space (U) of Bowman's capsule. Proximal (P) and distal (D) convoluted renal tubules showing normal epithelial lining and interstitial tissue. (Scale bar:10 µm).

Furthermore, histopathological examination of kidney section revealed no histological changes in the treated mice groups and were identical to control tissue sections (Fig. 10E). Perhaps this may be due to the nephroprotective properties of selenium nanoparticles [54].

4. Conclusion

In the current study, marine bacterial strain was isolated from beach sand of Mediterranean Sea. Based on 16S rRNA gene sequencing, the isolated strain was identified as *Bacillus halotolerance*. The results presented in this work demonstrate that cell free extract of *Bacillus halotolerance* could be used as an eco-friendly method to obtain spherical shaped SeNPs with diameter between 7.50-19.17 nm. The biosynthesized SeNPs were characterized and confirmed by UV–Vis spectroscopy, SEM–EDX, zeta potential, XRD and TEM techniques. We report for the first time, to our knowledge, statistical optimization of SeNPs biosynthesis by marine bacterium *Bacillus halotolerance* using Plackett–Burman Design. Moreover, we evaluate the acute and subacute toxicity of biosynthesized SeNPs in mice to screen its safety. The findings of the present study proved that biosynthesized SeNPs did not cause mortality in vivo up to a dose of 2000 mg/kg in an acute toxicity test. Moreover, SeNPs has no sub-acute toxicity as supported by biochemical, hematological and histological findings. Thus, the isolated bacterial strain can be exploited as a prospective, renewable, nanofactory for the biosynthesis of SeNPs which could be used safely as anticancer agent without any toxic risk.

5. Conflict of Interests

The authors declare that they have no competing interests.

6. Funding

Open access funding provided by The Science, Technology & Innovation Funding Authority (STDF) in cooperation with The Egyptian Knowledge Bank (EKB). Open access funding provided by The Science, Technology & Innovation Funding Authority (STDF) in cooperation with The Egyptian Knowledge Bank (EKB).

7. Acknowledgement

This study is supported by the National Research Centre, Egypt. Proteome research laboratory.

8. References

1. Zhang, T. *et al.* Recent research progress on the synthesis and biological effects of selenium nanoparticles. *Front. Nutr.* **10**, (2023).
2. Zhang, Z., Du, Y., Liu, T., Wong, K. H. & Chen, T. Systematic acute and subchronic toxicity evaluation of polysaccharide–protein complex-functionalized selenium nanoparticles with anticancer potency. *Biomater. Sci.* **7**, 5112–5123 (2019).
3. Emam, H. E., Zaghloul, S. & Ahmed, H. B. Full ultraviolet shielding potency of highly durable cotton via self- implantation of palladium nanoclusters. *Cellulose* **29**, 4787–4804 (2022).
4. Ali, H. O. *et al.* Simulated and experimental studies of a multi-band symmetric metamaterial absorber with polarization independence for radar applications. *Chinese Phys. B* **31**, 058401 (2022).
5. Karatepe, A. *et al.* A monopole microwave-assisted electrochemical sensor for the detection of liquid chemicals. *Dig. J. Nanomater. Biostructures* **16**, 765–776
6. Djanaguiraman, M., Belliraj, N., Bossmann, S. H. & Prasad, P. V. V. High-Temperature Stress Alleviation by Selenium Nanoparticle Treatment in Grain Sorghum. *ACS omega* **3**, 2479–2491 (2018).
7. Shahabadi, N., Zendehcheshm, S. & Khademi, F. Selenium nanoparticles: Synthesis, in-vitro cytotoxicity, antioxidant activity and interaction studies with ct-DNA and HSA, HHb and Cyt c serum proteins. *Biotechnol. reports (Amsterdam, Netherlands)* **30**, (2021).
8. Emam, H. E., Mikhail, M. M., El-Sherbiny, S., Nagy, K. S. & Ahmed, H. B. Metal-dependent nano-catalysis in reduction of aromatic pollutants.

Environ. Sci. Pollut. Res. **27**, 6459–6475 (2020).
9. Khurana, A., Tekula, S., Saifi, M. A., Venkatesh, P. & Godugu, C. Therapeutic applications of selenium nanoparticles. *Biomed. Pharmacother.* **111**, 802–812 (2019).
10. Bano, I., Skalickova, S., Arbab, S., Urbankova, L. & Horky, P. Toxicological effects of nanoselenium in animals. *J. Anim. Sci. Biotechnol.* **13**, 1–13 (2022).
11. Nayak, V., Singh, K. R., Singh, A. K. & Singh, R. P. Potentialities of selenium nanoparticles in biomedical science. *New J. Chem.* **45**, 2849–2878 (2021).
12. Ullah, A. *et al.* Biogenic Selenium Nanoparticles and Their Anticancer Effects Pertaining to Probiotic Bacteria-A Review. *Antioxidants (Basel, Switzerland)* **11**, (2022).
13. Bai, K., Hong, B., Huang, W. & He, J. Selenium-Nanoparticles-Loaded Chitosan/Chitooligosaccharide Microparticles and Their Antioxidant Potential: A Chemical and In Vivo Investigation. *Pharm. 2020, Vol. 12, Page 43* **12**, 43 (2020).
14. Song, X. *et al.* Preparation, characterization, and in vivo evaluation of anti-inflammatory activities of selenium nanoparticles synthesized by Kluyveromyces lactis GG799. *Food Funct.* **12**, 6403–6415 (2021).
15. Sonkusre, P. Specificity of Biogenic Selenium Nanoparticles for Prostate Cancer Therapy With Reduced Risk of Toxicity: An in vitro and in vivo Study. *Front. Oncol.* **9**, 492150 (2020).
16. Xiao, Y., Huang, Q., Zheng, Z., Guan, H. & Liu, S. Construction of a Cordyceps sinensis exopolysaccharide-conjugated selenium nanoparticles and enhancement of their antioxidant activities. *Int. J. Biol. Macromol.* **99**, 483–491 (2017).
17. Staicu, L. C. *et al.* Interplay between arsenic and selenium biomineralization in Shewanella sp. O23S. *Environ. Pollut.* **306**, 119451 (2022).
18. Hosnedlova, B. *et al.* Nano-selenium and its nanomedicine applications: a critical review. *Int. J. Nanomedicine* **13**, 2107–2128 (2018).
19. Zambonino, M. C. *et al.* Green Synthesis of Selenium and Tellurium Nanoparticles: Current Trends, Biological Properties and Biomedical Applications. *Int. J. Mol. Sci.* **22**, 1–34 (2021).
20. Chopra, H. *et al.* Green Metallic Nanoparticles: Biosynthesis to Applications. *Front. Bioeng. Biotechnol.* **10**, (2022).
21. Husen, A. & Siddiqi, K. S. Plants and microbes assisted selenium nanoparticles: Characterization and application. *J. Nanobiotechnology* **12**, 1–10 (2014).
22. Tugarova, A. V. & Kamnev, A. A. Proteins in microbial synthesis of selenium nanoparticles. *Talanta* **174**, 539–547 (2017).
23. Wang, Z. *et al.* Optimization of fermentation parameters to improve the biosynthesis of selenium nanoparticles by Bacillus licheniformis F1 and its comprehensive application. *BMC Microbiol.* **24**, (2024).
24. Alam, H. *et al.* Synthesis of Selenium Nanoparticles Using Probiotic Bacteria Lactobacillus acidophilus and Their Enhanced Antimicrobial Activity Against Resistant Bacteria. *J. Clust. Sci.* **31**, 1003–1011 (2020).
25. Stabnikova, O., Khonkiv, M., Kovshar, I. & Stabnikov, V. Biosynthesis of selenium nanoparticles by lactic acid bacteria and areas of their possible applications. *World J. Microbiol. Biotechnol. 2023 399* **39**, 1–20 (2023).
26. Ullah, A. *et al.* Biosynthesis of Selenium Nanoparticles (via Bacillus subtilis BSN313), and Their Isolation, Characterization, and Bioactivities. *Molecules* **26**, (2021).
27. Beleneva, I. A. *et al.* Biogenic synthesis of selenium and tellurium nanoparticles by marine bacteria and their biological activity. *World J. Microbiol. Biotechnol.* **38**, (2022).
28. Ashengroph, M. & Hosseini, S. R. A newly isolated Bacillus amyloliquefaciens SRB04 for the synthesis of selenium nanoparticles with potential antibacterial properties. *Int. Microbiol.* **24**, 103–114 (2021).
29. Staicu, L. C. *et al.* Pseudomonas moraviensis subsp. stanleyae, a bacterial endophyte of hyperaccumulator Stanleya pinnata, is capable of efficient selenite reduction to elemental selenium under aerobic conditions. *J. Appl. Microbiol.* **119**, 400–410 (2015).
30. Fernández-Llamosas, H., Castro, L., Blázquez, M. L., Díaz, E. & Carmona, M. Speeding up bioproduction of selenium nanoparticles by using Vibrio natriegens as microbial factory. *Sci. Reports 2017 71* **7**, 1–9 (2017).
31. Joardar, S., Ray, S., Samanta, S. & Bhattacharjee, P. Antibacterial activity of 3,6-di(pyridin-2-yl)-1,2,4,5-s-tetrazine capped Pd(0) nanoparticles against Gram-positive Bacillus subtilis bacteria. *Cogent Biol.* **2**, 1249232 (2016).
32. Hassabo, A. A., Ibrahim, E., Ali, B. & Emam, H. E. Anticancer effects of biosynthesized Cu2O nanoparticles using marine yeast. *Biocatal. Agric. Biotechnol.* **39**, 102261 (2022).
33. Tamura, K., Dudley, J., Nei, M. & Kumar, S. MEGA4: Molecular Evolutionary Genetics Analysis (MEGA) Software Version 4.0. *Mol. Biol. Evol.* **24**, 1596–1599 (2007).
34. Abdelraof, M., Hasanin, M. S. & El-Saied, H. Ecofriendly green conversion of potato peel wastes to high productivity bacterial cellulose. *Carbohydr. Polym.* **211**, 75–83 (2019).
35. Habriev, R. U. *Guideline for Experimental (Preclinical) Studying of New Pharmacological Substances*. (Medicine, 2005).
36. Suvarna, S. K., Layton, C. & Bancroft, J. D. Bancroft's Theory and Practice of Histological Techniques, Eighth Edition. *Bancroft's Theory Pract. Histol. Tech. Eighth Ed.* 1–557 (2018). doi:10.1016/C2015-0-00143-5
37. Cremonini, E. *et al.* Biogenic selenium nanoparticles: characterization, antimicrobial activity and effects on human dendritic cells and fibroblasts. *Microb. Biotechnol.* **9**, 758 (2016).
38. Akçay, F. A. & Avcı, A. Effects of process conditions and yeast extract on the synthesis of selenium nanoparticles by a novel indigenous isolate Bacillus sp. EKT1 and characterization of nanoparticles. *Arch. Microbiol.* **202**, 2233–2243 (2020).

39. Shakibaie, M., Khorramizadeh, M. R., Faramarzi, M. A., Sabzevari, O. & Shahverdi, A. R. Biosynthesis and recovery of selenium nanoparticles and the effects on matrix metalloproteinase-2 expression. *Biotechnol. Appl. Biochem.* **56**, 7–15 (2010).
40. Kora, A. J. Bacillus cereus, selenite-reducing bacterium from contaminated lake of an industrial area: a renewable nanofactory for the synthesis of selenium nanoparticles. *Bioresour. Bioprocess.* **5**, 1–12 (2018).
41. Gunti, L., Dass, R. S. & Kalagatur, N. K. Phytofabrication of selenium nanoparticles from emblica officinalis fruit extract and exploring its biopotential applications: Antioxidant, antimicrobial, and biocompatibility. *Front. Microbiol.* **10**, 451408 (2019).
42. Ullah, A. *et al.* Biosynthesis of Selenium Nanoparticles (via Bacillus subtilis BSN313), and Their Isolation, Characterization, and Bioactivities. *Molecules* **26**, (2021).
43. Ruiz Fresneda, M. A. *et al.* Green synthesis and biotransformation of amorphous Se nanospheres to trigonal 1D Se nanostructures: impact on Se mobility within the concept of radioactive waste disposal. *Environ. Sci. Nano* **5**, 2103–2116 (2018).
44. Lian, S. *et al.* Characterization of biogenic selenium nanoparticles derived from cell-free extracts of a novel yeast Magnusiomyces ingens. *3 Biotech* **9**, 1–8 (2019).
45. Wadhwani, S. A. *et al.* Green synthesis of selenium nanoparticles using Acinetobacter sp. SW30: optimization, characterization and its anticancer activity in breast cancer cells. *Int. J. Nanomedicine* **12**, 6841–6855 (2017).
46. Fernández-Llamosas, H., Castro, L., Blázquez, M. L., Díaz, E. & Carmona, M. Biosynthesis of selenium nanoparticles by Azoarcus sp. CIB. *Microb. Cell Fact.* **15**, 1–10 (2016).
47. United Nations Economic Commission for Europe. *THE GLOBALLY HARMONIZED SYSTEM OF CLASSIFICATION AND LABELLING OF CHEMICALS*. (2005).
48. Ruswandi, Y. A. R. *et al.* Understanding the Roles of Selenium on Thyroid Hormone-Induced Thermogenesis in Adipose Tissue. *Biol. Trace Elem. Res.* **202**, 2419–2441 (2024).
49. Bizerea-Moga, T. O., Pitulice, L., Bizerea-Spiridon, O. & Moga, T. V. Exploring the Link between Oxidative Stress, Selenium Levels, and Obesity in Youth. *Int. J. Mol. Sci. 2024, Vol. 25, Page 7276* **25**, 7276 (2024).
50. Kaushal, N., Hegde, S., Lumadue, J., Paulson, R. F. & Prabhu, K. S. The regulation of erythropoiesis by selenium in mice. *Antioxid. Redox Signal.* **14**, 1403–1412 (2011).
51. Zhang, J. *et al.* Selenium Improves Bone Microenvironment-Related Hematopoiesis and Immunity in T-2 Toxin-Exposed Mice. *J. Agric. Food Chem.* **71**, 2590–2599 (2023).
52. Hamza, R. Z., EL-Megharbel, S. M., Altalhi, T., Gobouri, A. A. & Alrogi, A. A. Hypolipidemic and hepatoprotective synergistic effects of selenium nanoparticles and vitamin. E against acrylamide-induced hepatic alterations in male albino mice. *Appl. Organomet. Chem.* **34**, e5458 (2020).
53. Li, B. *et al.* Selenium-Alleviated Hepatocyte Necrosis and DNA Damage in Cyclophosphamide-Treated Geese by Mitigating Oxidative Stress. *Biol. Trace Elem. Res.* **193**, 508–516 (2020).
54. Li, S., Dong, X., Xu, L. & Wu, Z. Nephroprotective Effects of Selenium Nanoparticles Against Sodium Arsenite-Induced Damages. *Int. J. Nanomedicine* **18**, 3157 (2023).